

## Innovative Approach towards the Synthesis of Carbon Nanotubes from Natural Gas Using Iron Doped Red Mud

<sup>1</sup>Muhammad Bilal\*, <sup>2</sup>Tariq Mahmood, <sup>1</sup>Javed Ali and <sup>1</sup>Fozia Sultana

<sup>1</sup>Department of Chemistry, Kohat University of Science & Technology,  
Kohat-26000 (Khyber Pakhtunkhwa) Pakistan.

<sup>2</sup>National Centre for Physics, Quaid-e- Azam University, Islamabad, Pakistan.

bilalazim4@yahoo.co.uk\*

(Received on 29<sup>th</sup> November 2017, accepted in revised form 5<sup>th</sup> May 2018)

**Summary:** Red mud is a waste product of aluminum industry, produced during Bayer process. It mainly contains iron, potassium, aluminum and zinc. Currently, it is being used for the synthesis of carbon nanotubes. However, red mud, obtained from different ores, has diverse effects on the size of carbon nanotubes. Therefore, this work represents the composition of red mud produced in Pakistan. The effect of different iron concentration in red mud, on the synthesis of CNTs, was studied. Proton Induced X-rays emission was carried out to investigate the elements present in raw red mud. X-rays Diffraction crystallography of raw red mud showed that red mud had a mixture of quartz, hematite, goethite and hydro-garnet etc. Fourier Transform Infrared Spectroscopic studies gave stretching and bending vibration of OH bound to Fe, Al, and Si-O vibration. Carbon nanotubes were synthesized, using different reaction conditions i.e. temperature, un-doped and doped red mud. Methane was used as a source for carbon nanotubes. The reaction was carried out in a tube furnace over undoped and iron doped red mud separately. Scanning electron microscopy showed that CNTs with reduced sizes were observed on iron doped red mud.

**Keywords:** Red Mud, Carbon Nanotubes, Pakistani Natural gas, Chemical Vapor Deposition.

### Introduction

Industrial revolution has brought tremendous changes and advancement in world, in 21<sup>st</sup> century. However, at the same time, it has also brought a drastic environmental pollution, due to increasing amount of wastes, and hazardous discharged into environment [1, 2]. Red mud is a waste product, produced, during the preparation of aluminum from bauxite ore in the Bayer process [3-6]. It is highly alkaline due to the presence of oxides and hydroxides of alkali and alkaline earth metals, so it creates serious environmental problems when stockpiled into an open yard. Exposure to red mud can cause serious diseases of skin and eyes and thus it can affect the growth of crop [7]. Beside environmental impacts, red mud is accountable for a large number of applications, in the field of research, due to the presence of other components of interest and their use in the relevant area. The major components of red mud are iron, calcium, sodium, potassium, aluminum and silicon etc [6, 8]. Due to the presence of Fe and Ni, in red mud, researchers have taken keen interest in its use for different purposes. The catalytic role of Fe for the synthesis of CNTs, using Fe catalyst, are well known and studied by several researchers [9, 10]. These metals are known to be the most active catalysts for the decomposition of hydrocarbons [11]. Red mud and their pretreated forms have been used as a catalyst for hydrogenation, hydrodechlorination and oxidation of hydrocarbon [11-17]. In terms of oxidation, interest has been shown in the catalytic cracking of methane [17].

The overwhelming interest in catalytic cracking of methane is to reduce the hazardous effects of methane, because it is known to be about 23 times more potent as a greenhouse gas rather than CO<sub>2</sub>. It is often the undesirable end product of landfill dumping and refinery operation where in the latter case, it is flared [18]. One potential route, for methane, consumption is its catalytic cracking where it leads to the formation of carbon and H<sub>2</sub> both [19]. Although, this reaction is less efficient, but the use of iron, as a catalyst, enhanced the efficacy to a higher amount of product formation, and hence it proved the best activity of iron for this reaction [20, 21]. Carbon nanotubes were synthesized by Oscar *et al.* [9], using red, mud as a catalyst. It was observed that the red mud used for CNTs synthesis, using fluidized bed chemical vapor deposition method, appeared to be a 'ready-made' CNT catalyst, as its Fe composition is similar to several supported CNTs catalysts reported in the literature [9, 22]. Moreover, CNTs are unique and flexible adsorbents because these have wide surface area, its micro porous structure, and high adsorption capacity; but its high cost limits their use [23]. Hence, its production from low cost materials is important, and it gained considerable attention for waste water treatment in developing countries. Various researchers have synthesized CNTs from red mud by fluidized bed chemical vapor deposition (FCVD) [24].

CVD is comparatively simple and cost-effective technique, used for the synthesis of carbon

---

\*To whom all correspondence should be addressed.

nanotubes, as compared to arc-discharge and laser ablation methods [25]. CVD requires low temperature and ambient pressure to establish and this method suggests larger yield, high purity, and improved control of the structure and growth parameters. It is a cost effective method for the synthesis of highly good quality CNTs and it has the potential to upgrade the CNTs production on a commercial level [25]. The aim of this work was therefore to check the role of red mud of Pakistan Aluminum industry as a catalyst for the synthesis of carbon nanotubes, using effluent gas, coming out from natural gas well in Pakistan. This work represents that how the different concentration of iron content, in red mud, influence the morphology of CNTs.

### Experimental

Raw red mud was collected from Aluminum processing industries, international S.I.T.E, Karachi, Sind, Pakistan (Fig. 1). Raw sample was dried in an oven at 105°C overnight and the dried sample was ground. The ground red mud was sieved and obtained particle (200-450 micrometer). This sample was characterized using PIXE, XRD, Raman and FTIR in order to investigate composition of raw red mud, phase studies, and functional group analysis. Proton Induced X-ray Emission can be used for simultaneous examination of 72 inorganic elements from Sodium, through Uranium, on the Periodic Table in different states (solid, liquid and thin film) of samples [26]. FTIR Bruker, Pensor 27 was used for functional group analysis. The sample was analyzed in argon atmosphere and the temperature was kept in the range of 19-25°C and. Functional groups were analyzed in term of wave number ranging from 4000-400cm<sup>-1</sup> using KBr method. D8 advanced Bruker X-ray diffractometer was used for phase change and crystallographic studies of raw red mud and red mud being carbonized in different conditions. Cu K $\alpha$  radiation,  $\lambda = 1.54 \text{ \AA}$  was used for X-Ray production. From the XRD patterns, grain size for various phases was calculated, using Debye-Scherrer formula (Using  $K = 1$ ). SEM images were taken using MIRA3 TESCAN (100 kx and 10 keV). In SEM, electron beam was produced by tungsten filament. The sample was analyzed without gold plating. Raman spectra of catalysts were obtained with a Horiba Jobin Yvon LabRAM High Resolution spectrometer. A 532.17 nm line of a coherent Kimmon IK series He-Cd laser was used as the excitation source for the laser. A scanning range of between 100 and 4100 cm<sup>-1</sup> was applied.

For preparation of 5% Iron doped red mud, 2.2g of iron nitrate was dissolved in a minimum quantity of distilled water and then it was sprayed on 9.5g of raw red mud. After spraying iron nitrate on red mud, the sample was dried in an oven for 24 hrs, and then

calcined up to 800°C in nitrogen atmosphere. Similarly 10% Iron doped Red mud was prepared using the same procedure as discussed above.

Chemical vapor deposition method was used for the synthesis of CNTs, from natural, gas using gas flow of 40ml/min. The reaction was carried out in a quartz tube fitted inside the furnace. The natural gas, used, was obtained from well in KPK, Pakistan, without any further purification. The natural gas was mixed with nitrogen in a ratio of 1:1. The reaction was performed at two different temperatures i.e. 650°C and 700°C. The CNTs synthesis was checked on both raw and iron doped red mud at 700°C. Synthesized carbonized red mud was characterized using XRD, SEM in order to investigate the formation of CNTs.

### Results and Discussion

#### Proton induced X-ray Emission Analysis

Table-1 shows that Iron is present in the highest quantity i.e. 52.59 %, of the total 11 elements in red mud of Pakistan. Its quantity is comparable with chemical composition of red mud collected from different countries and compatible for CNTs synthesis with different supported catalysts since used for CNTs synthesis [27, 28].

Table-1: Element present in raw red mud and their weight percent composition.

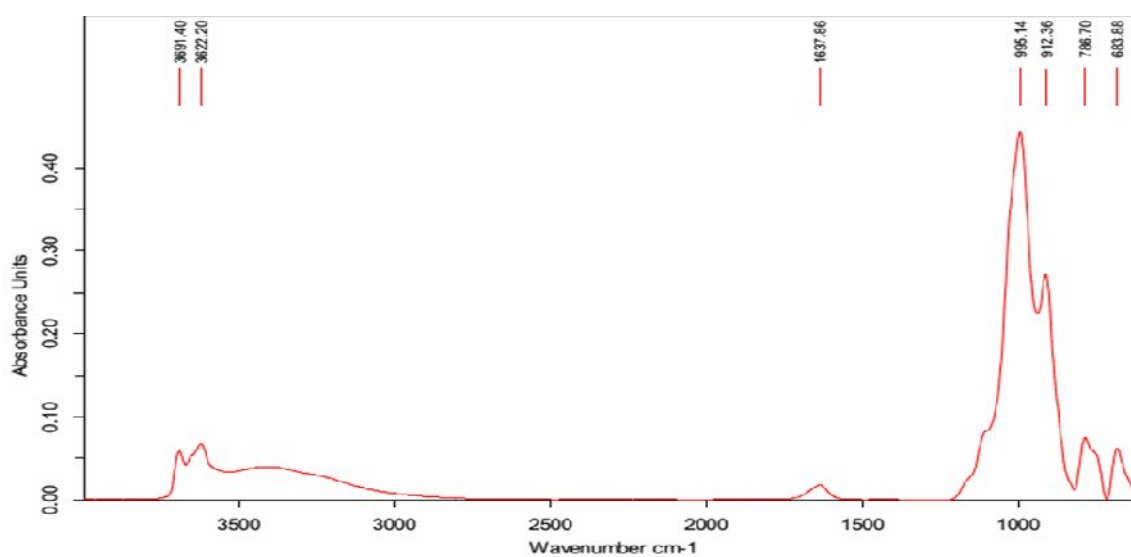
Element	% Composition	Element	% Composition
Fe	52.59	Ti	0.42
K	26.64	Ni	0.11
Ca	9.01	Co	0.08
Zn	6.76	Cu	0.04
Si	0.89	Cr	0.003
Mn	0.83		

#### Comparison of FTIR Analysis of Raw Red Mud, 5% and 10% Iron doped Red Mud

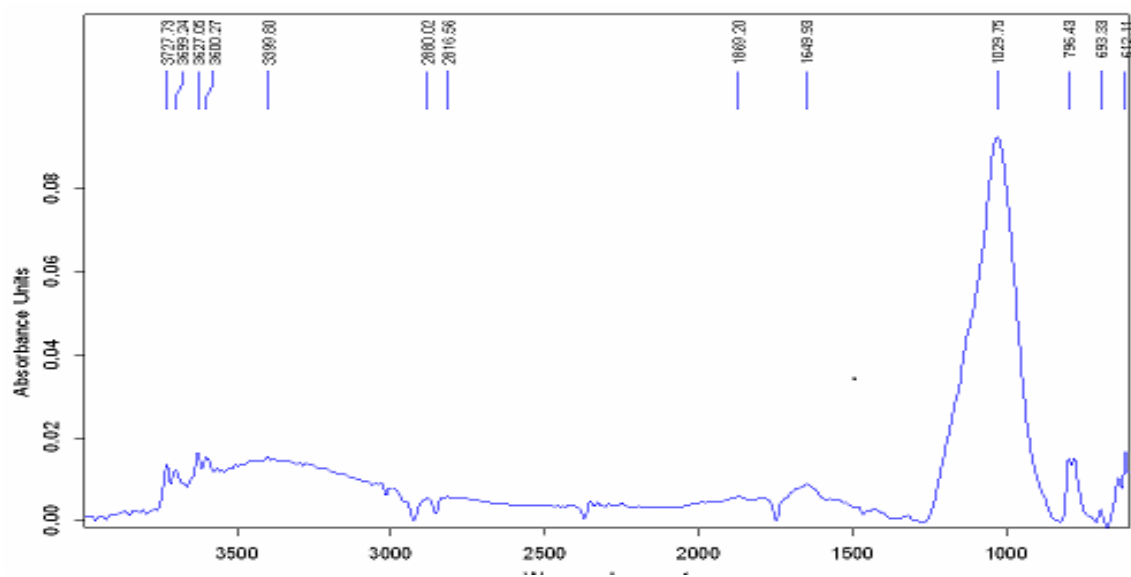
All the absorption peaks of raw red mud are shown in Fig. 2 (a). It is reported that rutile give a characteristic band at 683 cm<sup>-1</sup> and absorption at 3622cm<sup>-1</sup> which is corresponding to Al-OH stretching vibration [29]. The band at 996.14 cm<sup>-1</sup> is reported for the stretching vibration of Si (Al)-O [30]. Stretching vibration of Fe-O is reported at 1637cm<sup>-1</sup> [31]. The band at 3692 cm<sup>-1</sup> represent the O-H stretching vibration in kaolinite and the peak at position 912cm<sup>-1</sup> represent O-H bending vibration [32]. The band at 1637 cm<sup>-1</sup> corresponds to the bending vibrations of interlayer absorbed water molecule. Fig. 2 (b and c) shows that the bands at position 796 cm<sup>-1</sup> represents Fe-O stretching vibration of the maghmite [33]. This band is present in both 5% and 10% iron doped red mud.



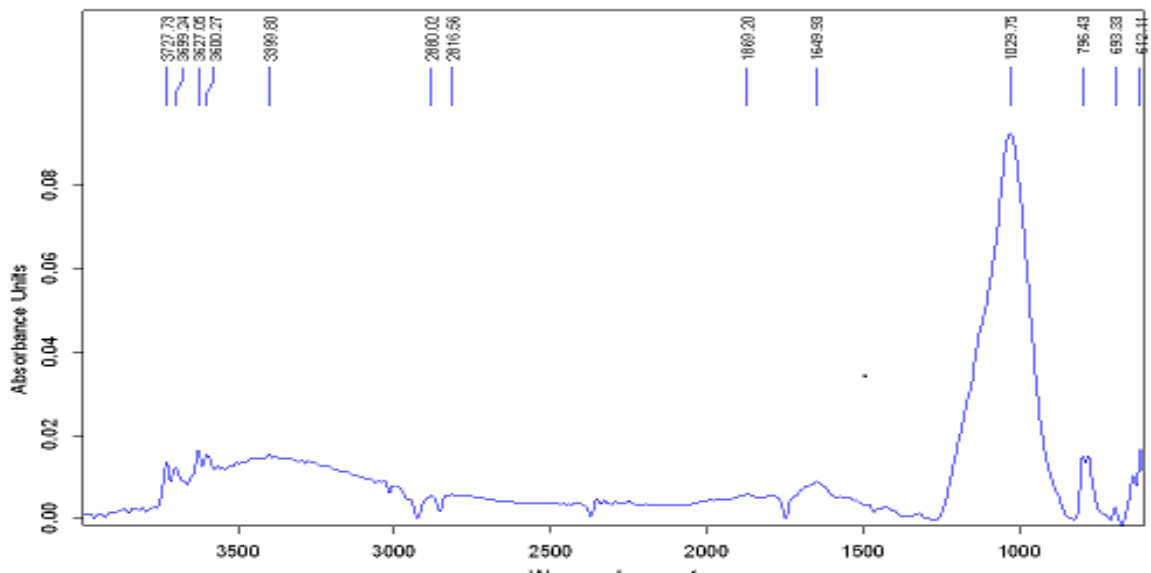
Fig. 1: cakes of dried raw red mud.



(A)



(B)



(C)

Fig. 2: FTIR spectra of (a) raw red mud, (b) 5% iron doped red mud, and (c) 10% iron doped red mud.

#### XRD Analysis of Raw Red Mud and Carbonized Red Mud:

Fig. 3 represents the X-rays crystallographic study of raw red mud and carbonized red mud. The most intense peak, present in the XRD patterns of raw red mud, is iron silicate hydroxide at a  $2\theta$  of 26. The XRD patterns of raw red mud also represents many low and high intensity peaks for hematite phase shown in Fig. 3 [31, 34-36].

The morphology and phase studies of red mud, being carbonized using various conditions, are given in Fig. 3. The XRD patterns of raw red mud on exposure to methane at  $650^\circ\text{C}$  is identical to XRD of raw red mud, while, at  $700^\circ\text{C}$ , the deposition of carbon on red mud occurred, according to literature the peak at  $2\theta$  of 26 is now correspond to minnesotaite and graphite [36]. On comparison, the XRD of red mud carbonized at  $700^\circ\text{C}$  showed a decrease in the crystallinity of minnesotaite phase which mean that the deposit carbon suppress the crytallinity of mannisotaite. The peak intensity at  $2\theta$  of 26 is even lower in 5% and 10% iron doped carbonized red mud at  $700^\circ\text{C}$  showed that carbon deposition suppress the crystalliniy of various phases. The peak at  $2\theta$  43 now represents the Fe in Fig. 3(c) [26].

#### SEM images of Carbonized Red Mud

The comparison of SEM images of red mud carbonized at various temperatures is given in Fig. 4 and Fig. 5. It illustrates that at  $650^\circ\text{C}$  when the raw red mud was exposed to natural gas, the formation of CNTs was not observed, so, this result coincide with the XRD pattern of raw red mud at  $650^\circ\text{C}$  on exposure to natural gas. When reaction was performed at  $700^\circ\text{C}$  on raw red mud, CNTs of 50 nm in diameter appeared as shown in Fig. 5. This indicates that the minimum temperature required for the formation of CNTs on red mud is  $700^\circ\text{C}$  which is supported by previous Literature [36, 37]. Iron doped red mud was carbonized at  $700^\circ\text{C}$  which indicated that size of CNTs is decreased with increase in the concentration of the iron in red mud. The CNTs, synthesized at  $700^\circ\text{C}$  on raw red mud, have a diameter of 50nm and this result also justifies the XRD pattern of raw red mud on exposure to methane at the same temperature i.e. the graphitic phase was observed at  $700^\circ\text{C}$ . Doping has also a remarkable effect on the morphology of CNTs which is visible in Fig. 6 and Fig. 7. Number of CNTs increased with the increase of iron doping on red mud i.e. the number of CNTs is greater in 10% iron doped red mud than 5%. The amounts of CNTs are also significant in 5%, however not clearly visible in 5% iron doped red mud because of the low resolution of SEM used. It was also found that with the increased number of CNTs the size of CNT got an apparently reduced.

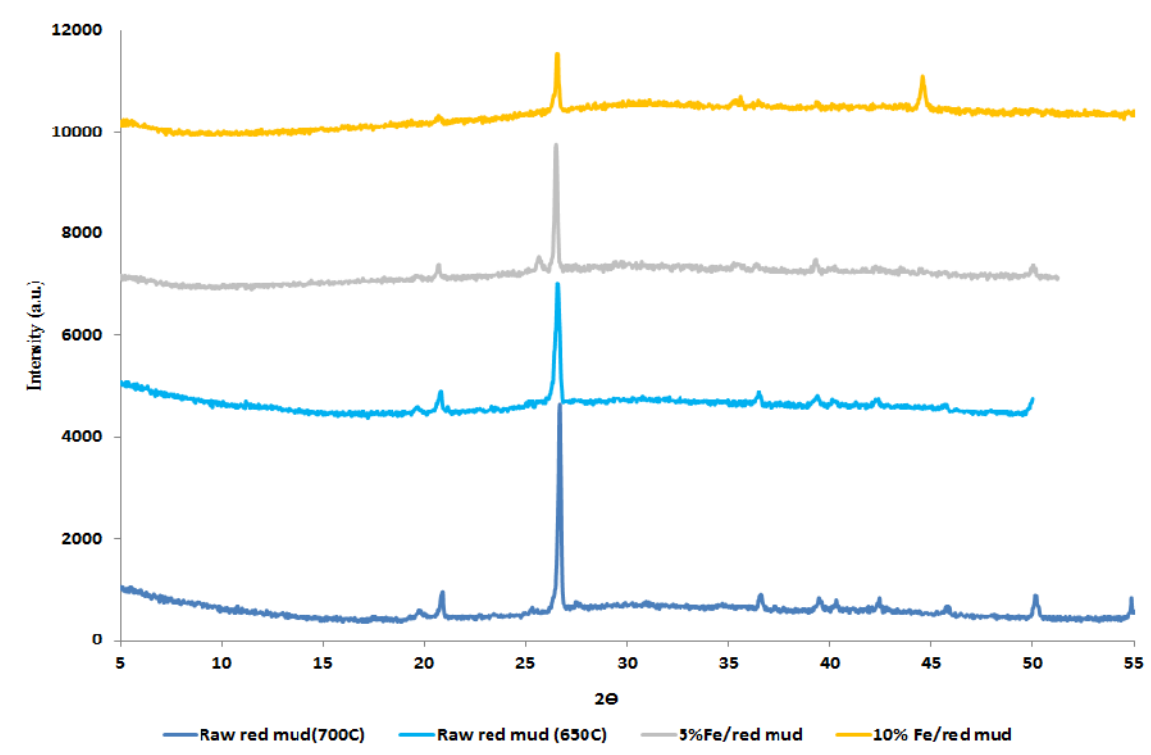


Fig. 3: XRD patterns of (A) raw red mud, (B) red mud carbonized at 650°C, (C) red mud carbonized at 700 °C, (D) 5% iron doped carbonized red mud and (E) 10% iron doped red mud

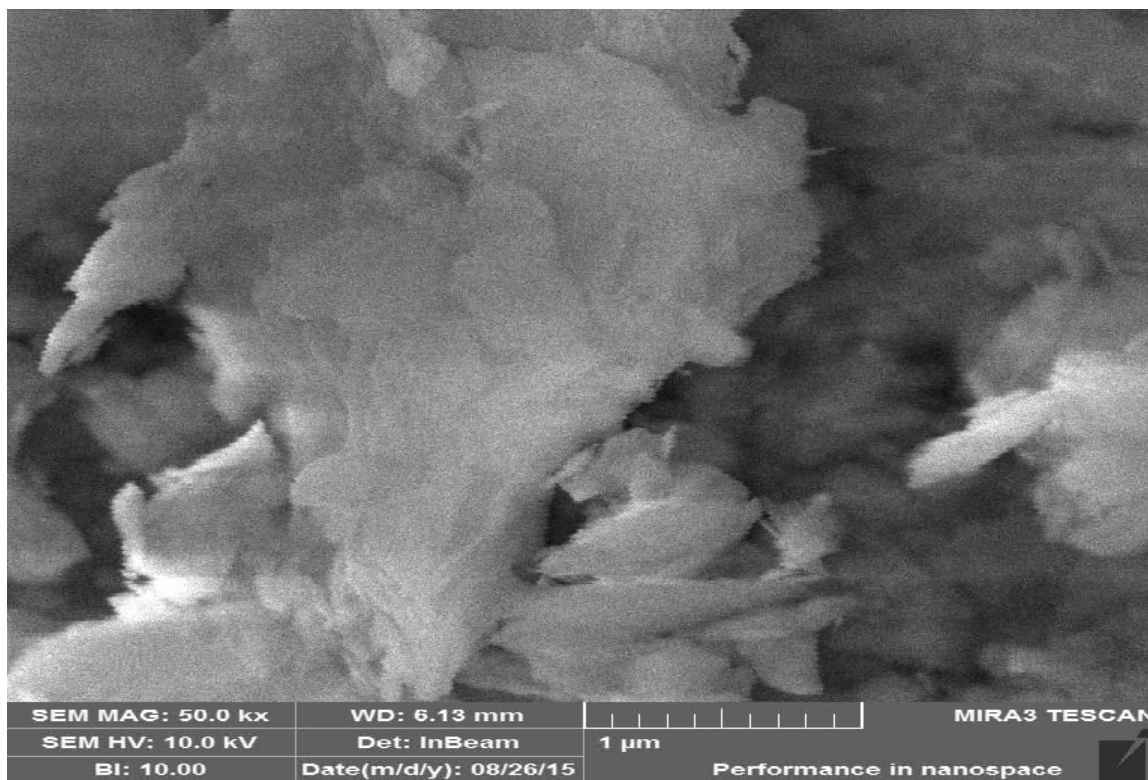


Fig. 4: Comparison of SEM images of carbonized red mud @ 650 °C.

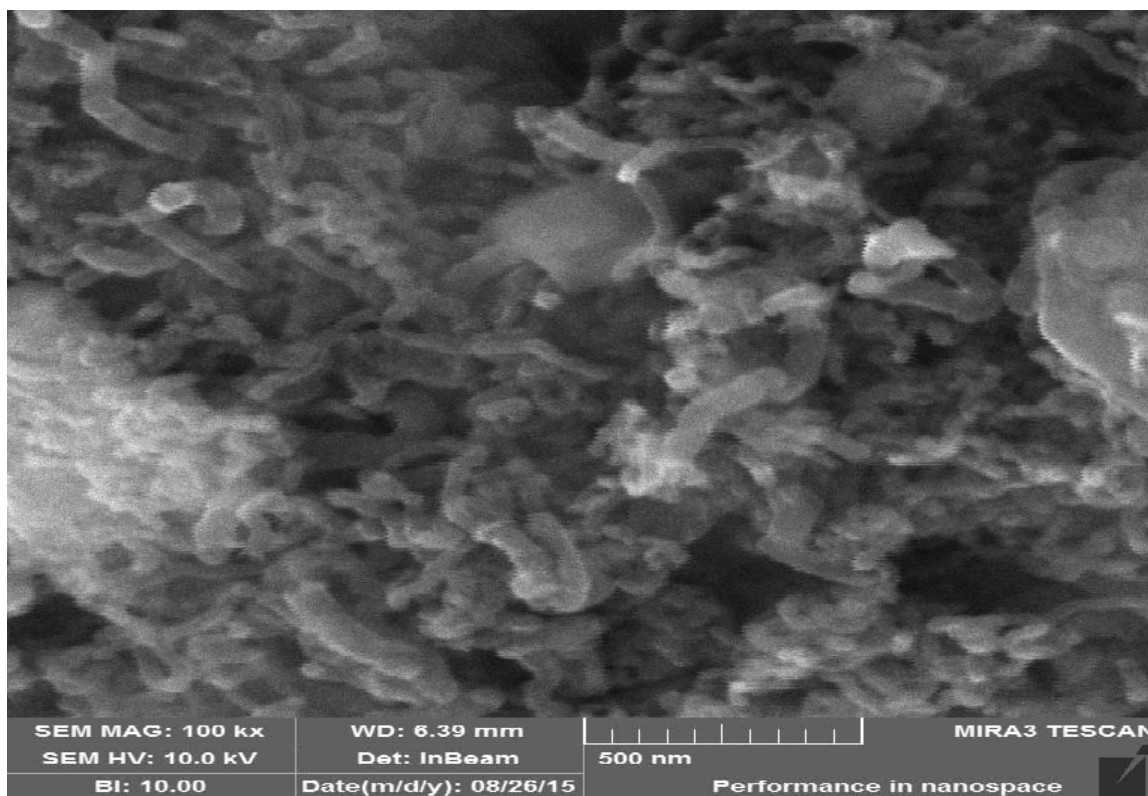


Fig. 5: Comparison of SEM images of carbonized red mud @ 700 °C.

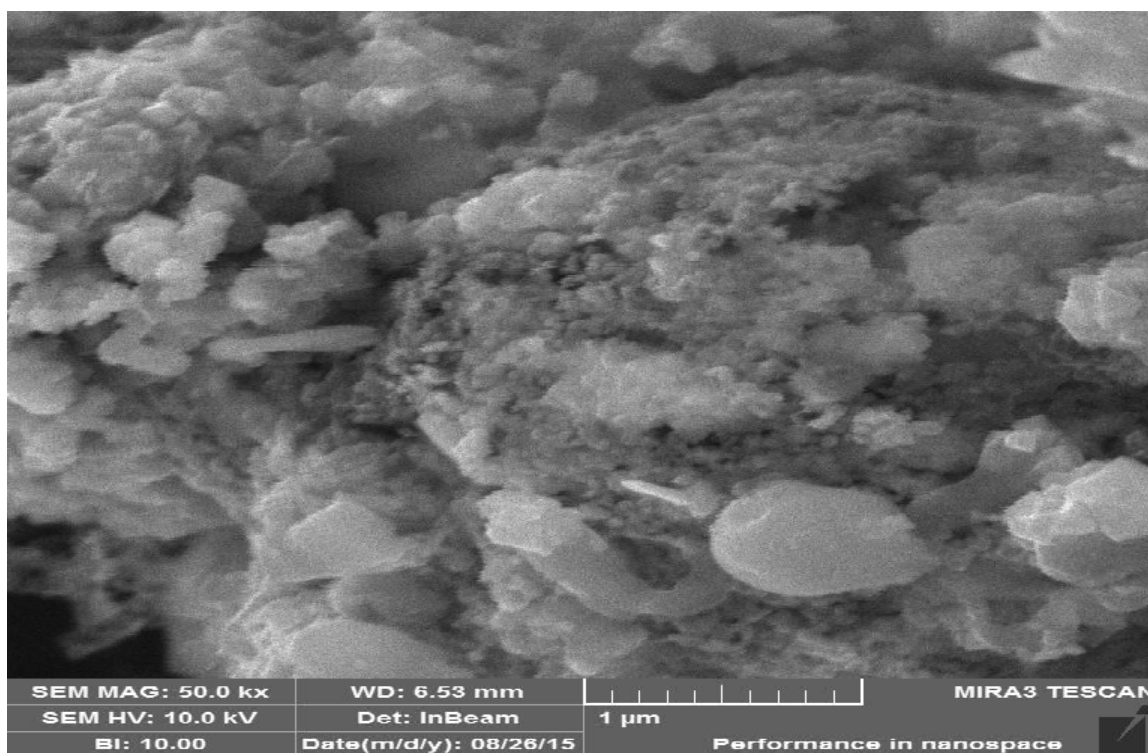


Fig. 6: Comparison of SEM images of carbonized 5% iron doped red mud.

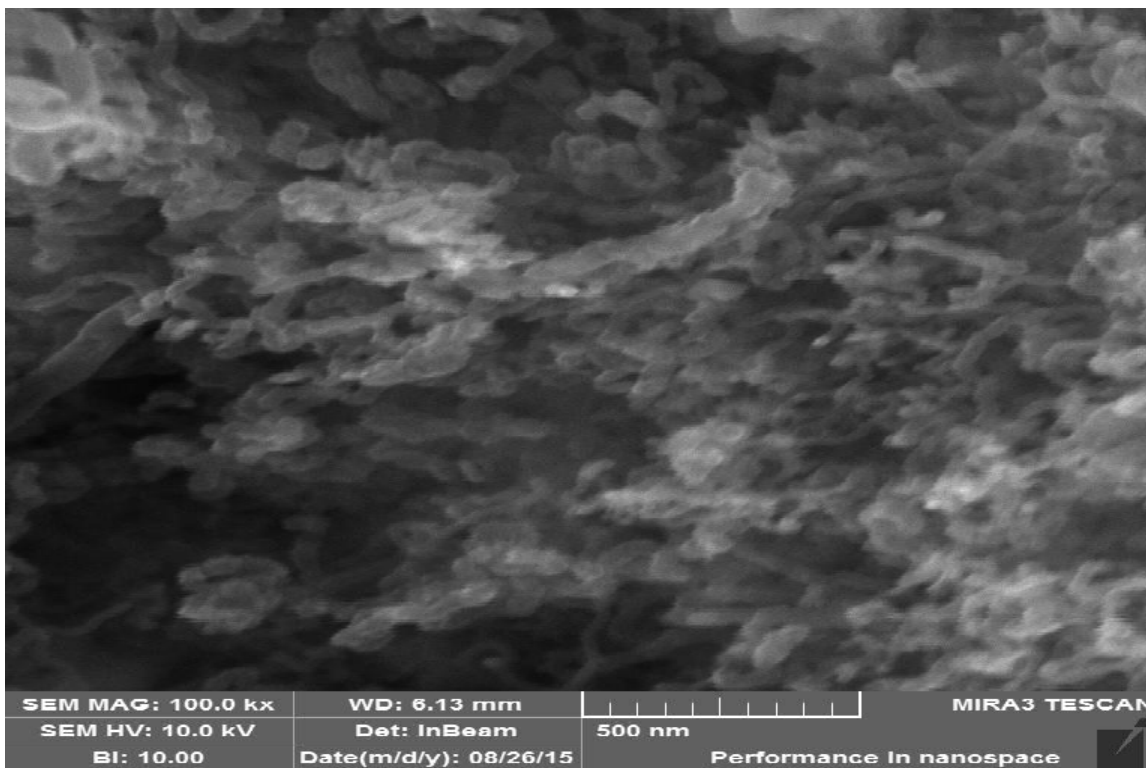


Fig. 7: Comparison of SEM images of carbonized 10% iron doped red mud.

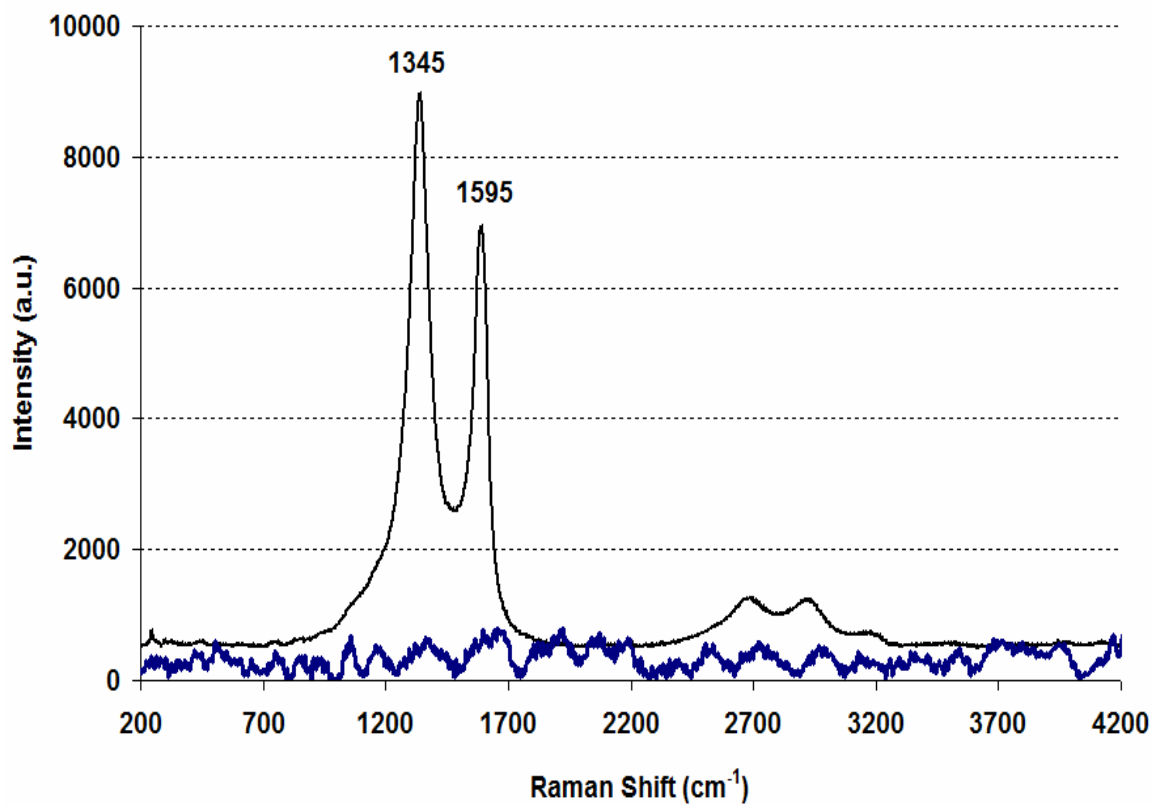


Fig. 8: Raman Analysis of carbonized red mud (a) at 650 °C (Blue) (b) at 700 °C (Black).

Table-2: Average crystallite size of raw red mud.

Phase	Average Crystallite size (nm)
Hematite( $\text{Fe}_2\text{O}_3$ )	110.00
Goethite( $\text{FeO}(\text{OH})$ )	7.80
Nepheline( $\text{NaK}(\text{AlSiO}_3)$ )	7.77

Table-3: Average crystallite size of raw red mud on exposure to methane at 650 °C.

Phase	Average Crystallite size(nm)
Hematite( $\text{Fe}_2\text{O}_3$ )	3.38
Goethite( $\text{FeO}(\text{OH})$ )	6.48
Nepheline( $\text{NaK}(\text{AlSiO}_3)$ )	5.18

Table-4: Average crystallite size of raw red mud on exposure to methane at 700 °C.

Phase	Average Crystallite size (nm)
Minnesotaite( $\text{Fe}^{2+}, \text{Mg}_3\text{Si}_4\text{O}_{10}(\text{OH})_2$ )	5.18
Hematite( $\text{Fe}_2\text{O}_3$ )	2.59
Graphitic carbon (C)	4.91

Table-5: CHN analysis of raw and iron doped red mud.

Catalyst Name	Temperature(°C)	Carbon	Hydrogen	Nitrogen
Raw red mud	650	15.25	0.67	0.0
	700	18.39	0.25	
5% Fe/red mud	700	27.65	0.15	0.0
10% Fe/red mud	700	30.27	0.20	0.0

The depositions of CNTs at different temperatures and on iron doped catalyst were further investigated by CHN analysis. CHN results indicate that the amount of CNTs deposition on catalysts increased with an increase of temperature as well as with doping of iron as shown in Table-5. These results support the formation of CNTs on catalysts surface which are seen in SEM images. Cracking of methane gave different types of coke. The Raman analyses further confirm that the depositions on catalysts are CNTs which are graphitic in nature. Fig. 8 indicates that at 500 °C no band is observed in Raman analysis while at 700 °C two bands are appeared which are matching with graphitic carbon bands [38].

## Conclusions

In this work, raw red mud, produced in Pakistan, was doped with iron and used for synthesis of CNTs from natural gas produced in Pakistani wells. From results, it was concluded that the red mud of Pakistan contains 11 elements and iron is present in highest amount i.e. 52%. The iron value of red mud enabled us to use this waste for the synthesis of carbon nanotubes because iron, and nickel are known to be the most active catalyst for CNTs synthesis. CNTs are synthesized at 700 °C on raw red mud and iron doped red mud. Formation of CNTs was confirmed by SEM, CHN and Raman analysis. The number of CNTs is increased while the size is apparently reduced with increasing iron doping of red mud. Hence, red mud showed a highest efficacy for carbon nanotubes synthesis, particularly 10% iron doped red mud.

## References

1. J. Okereke, O. Ogidi and K. Obasi, Environmental and Health Impact of Industrial Wastewater Effluents In Nigeria-A Review, *Int. J. Adv. Res. Biol. Sci.*, **3**, 55 (2016).
2. A. M. Kanashiro, and J. Xie, Evaluation of Chemical Properties of Dredged Materials, Paranagua Port, Brazil, According To Dredging Legislation Conama 454/2012, *Universal Journal of Management*, **4**, 246 (2016).
3. Q. Liu, H. Li, X. Fang, J. Zhang, C. Zhang, M. Ma, F. Li and G. Huang, Preparation of Modified Red Mud-Supported Fe Catalysts for Hydrogen Production by Catalytic Methane Decomposition, *Journal of Nanomaterials*, **2017**, 11 (2017).
4. K. Pirkanniemi and M. Sillanpää, Heterogeneous Water Phase Catalysis as An Environmental Application: A Review, *Chemosphere*, **48**, 1047 (2002).
5. J. Pascual, F. A. Corpas, J. López-Beceiro, M. Benítez-Guerrero and R. Artiaga, Thermal Characterization of A Spanish Red Mud, *Journal of Thermal Analysis and Calorimetry*, **96**, 407 (2009).
6. M. Ermakova, and D. Y. Ermakov, Ni/SiO<sub>2</sub> and Fe/SiO<sub>2</sub> Catalysts for Production of Hydrogen and Filamentous Carbon via Methane Decomposition, *Catalysis Today*, **77**, 225 (2002).
7. S. Muduli, P. Rout, S. Pany, S. Mustakim, B. Nayak, and B. Mishra, Innovative Process in Manufacture of Cold Setting Building Brick from Mining and Industrial Wastes, *Indian Min. Eng. J.*, **49**, 127 (2010).

8. N. Zhao, Q. Cui, C. He, C. Shi, J. Li, H. Li. and X. Du, Synthesis of Carbon Nanostructures with Different Morphologies by CVD of Methane, *Materials Science and Engineering: A*, **460**, 255 (2007).
9. K. Kouravelou, S. Sotirchos and X. Verykios, Catalytic Effects of Production of Carbon Nanotubes In A Thermogravimetric CVD Reactor, *Surface and Coatings Technology*, **201**, 9226 (2007).
10. S. Iijima, Single wall Carbon nanotubes of 1-nm diameter, *Nature*, **363**, 603 (1993).
11. A. Cunha, J. Órfão and J. Figueiredo, Catalytic Decomposition of Methane on Raney-Type Catalysts, *Applied Catalysis A: General*, **348**, 103 (2008).
12. J. Álvarez, S. Ordóñez, R. Rosal, H. Sastre and F.V. Díez, A New Method for Enhancing the Performance of Red Mud as A Hydrogenation Catalyst, *Applied Catalysis A: General*, **180**, 399 (1999).
13. J. Alvarez, R. Rosal, H. Sastre and F.V. Díez, Characterization and Deactivation Studies of an Activated Sulfided Red Mud Used as Hydrogenation Catalyst, *Applied Catalysis A: General*, **167**, 215 (1998).
14. S. Ordonez, H. Sastre and F. Díez, Deactivation of Red Mud and Modified Red Mud Used as Catalyst for the Hydrodechlorination of Tetrachloroethylene, *Studies in Surface Science and Catalysis*, **126**, 443 (1999).
15. S. Ordonez, H. Sastre and F. Díez, Catalytic Hydrodechlorination of Tetrachloroethylene Over Red Mud, *Journal of hazardous materials*, **81**, 103 (2001).
16. S. Ordonez, H. Sastre and F. Díez, Hydrodechlorination of Tetrachloroethylene Over Modified Red Mud: Deactivation Studies and Kinetics, *Applied Catalysis B: Environmental*, **34**, 213 (2001).
17. J. Paredes, S. Ordonez, A. Vega and F. Díez, Catalytic Combustion of Methane Over Red Mud-Based Catalysts, *Applied Catalysis B: Environmental*, **47**, 37 (2004).
18. I. Pulford and H. Flowers, Environmental chemistry at a glance, *Wiley-Blackwel*, London, p. 144 (2006).
19. T. Choudhary, and D. Goodman, Methane Decomposition: Production of Hydrogen and Carbon Filaments, *Catalysis*, **19**, 164 (2006).
20. S. Takenaka, M. Serizawa and K. Otsuka, Formation of Filamentous Carbons Over Supported Fe Catalysts through Methane Decomposition, *Journal of Catalysis*, **222**, 520 (2004).
21. A. Alharthi, R. A. Blackley T. H., Flowers, J. S. J. Hargreaves, I. D. Pulford, J. Wigzell and W. Zhou, Iron Ochre— A Pre-Catalyst for the Cracking of Methane, *Journal of Chemical Technology and Biotechnology*, **89**, 1317 (2014).
22. A. R. Harutyunyan, B. K. Pradhan, U. Kim, G. Chen and P. Eklund, CVD Synthesis of Single Wall Carbon Nanotubes Under “Soft” Conditions, *Nano letters*, **2**, 525 (2002).
23. B. M. Tyson, R. K. Abu Al-Rub, A. Yazdanbakhsh and Z. Grasley, Carbon Nanotubes and Carbon Nanofibers for Enhancing the Mechanical Properties Of Nanocomposite Cementitious Materials, *Journal of Materials in Civil Engineering*, **23**, 1028 (2011).
24. H. M. Khater, H. A. Abd and E. L. Gawaad, Characterization of Alkali Activated Geopolymer Mortar doped with MWCNT, *Advances in materials Research*, **4**, 45 (2015).
25. A. M. Hunashyal, S. V. Tippa, S. S. Quadri and N. R. Banapurmath, Experimental Investigation on Effect of Carbon Nanotubes and Carbon Fibres on the Behavior of Plain Cement Mortar Composite Round Bars under Direct Tension, *ISRN Nanotechnology*, **2011**, 6 (2011).
26. W. Reuter, A. Lurio, F. Cardone and J. Ziegler, Quantitative Analysis of Complex Targets by Proton-Induced X-Rays, *Journal of Applied Physics*, **46**, 3194 (1975).
27. S. Sushil and V. S. Batra, Catalytic Applications of Red Mud, an Aluminum Industry Waste: A Review, *Applied Catalysis B: Environmental*, **81**, 64 (2008).
28. R. Paramguru, P. Rath and V. Misra, Trends in Red Mud Utilization—A Review, *Mineral Processing & Extractive Metall. Rev.*, **26**, 1 (2004).
29. K. Sujatal, D. Singh, A. Mishra, M. Upadhyay and K. Saroj, Red Mud as Adsorbent to Remove Lead (II) from Aqueous Solutions, *Research Journal of Recent Sciences*, **3**, 18 (2014).
30. A. H. Bhat, H. P. S. A. Khalil, I. ul Haq Bhat and A. K. Banthia, Dielectric and Material Properties of Poly (Vinyl Alcohol): Based Modified Red Mud Polymer Nanocomposites, *Journal of Polymers and the Environment*, **20**, 395 (2012).
31. A. Pappu, M. Saxena and S. R. Asolekar, Solid Wastes Generation in India and their Recycling Potential in Building Materials, *Building and Environment*, **42**, 2311 (2007).
32. G. F. Wasse Bekele and N. Fernandez, Removal of Nitrate Ion from Aqueous Solution by Modified Ethiopian Bentonite Clay, *International Journal of Research in Pharmacy and Chemistry*, **4**, 192 (2014).

33. E. Darezereshki, One-Step Synthesis of Hematite ( $\text{A-Fe}_2\text{O}_3$ ) Nano-Particles by Direct Thermal-Decomposition of Maghemite, *Materials Letters*, **65**, 642 (2011).
34. E. Lombi, F.-J. Zhao, G. Zhang, B. Sun, W. Fitz, H. Zhang and S. P. McGrath, In Situ Fixation of Metals in Soils Using Bauxite Residue: Chemical Assessment, *Environmental pollution*, **118**, 435 (2002).
35. J. L. Cao, Z. L. Yan, Q.-F. Deng, Y. Wang, Z. Y. Yuan, G. Sun, T.-K. Jia, X.-D. Wang, H. Bala and Z. Y. Zhang, Mesoporous Modified-Red-Mud Supported Ni Catalysts for Ammonia Decomposition to Hydrogen, *International Journal of Hydrogen Energy*, **39**, 5747 (2014).
36. A. Collazo, A. Covelo and C. Pérez, Characterization of Hybrid Sol-Gel Films Doped with Red Mud Particles, *Surface and Interface Analysis*, **44**, 1177 (2012).
37. M. Ermakova, D. Y Ermakov, A. L. Chuvilin and G. G. Kuvshinov, Ni/SiO<sub>2</sub> and Fe/SiO<sub>2</sub> catalysts for production of hydrogen and filamentous carbon via methane decomposition, *Catalysis Today*, **77**, 225 (2002).
38. S. Reich and C. Thomsen, Raman Spectroscopy of Graphite, *Philosophical Transactions of the Royal Society A*, **362**, 2271 (2004).